Adaptive Motion Estimation for Image Sequences under Non-uniform Illumination Variations

Shang-Hong Lai

Department of Computer Science
National Tsing Hua University, Hsinchu, Taiwan, R.O.C.
Email: lai@cs.nthu.edu.tw

Abstract

In this paper, we present an adaptive and accurate motion estimation algorithm for computing optical flow from an image sequence. The proposed algorithm is based on a regularization formulation that minimizes a combination of a modified data-constraint energy and a smoothness measure all over the pixels in the image domain. Unlike the conventional gradient-based optical flow computation, the data constraint used in this paper is derived from the conservation of the Laplacian-of-Gaussian (LoG) filtered image intensity in the temporal sequence. This modification alleviates the problem with the brightness constancy assumption under non-uniform illumination variations due to the use of Laplacian-of-Gaussian filter to remove the low-frequency portion of the additive non-uniform illumination factor. The modified data constraint simply replaces the image intensity function in the image flow constraint by the LoG filtered intensity function. In addition, an adaptively weighted membrane smoothness constraint is employed in our regularization framework. The resulting energy minimization is accomplished by a incomplete Cholesky preconditioned conjugate gradient algorithm. Experimental results on synthetic and real image sequences for our algorithm are given to demonstrate its performance.

1 Introduction

Image motion analysis plays a central role in the research of computer vision. Optical flow is the correspondence for each pixel between two consecutive frames in an image sequence. The computation of optical flow from an image sequence provides very important information for motion analysis, including moving object detection, object tracking, moving object segmentation, and motion recognition. In addition, the computation of optical flow is essential for the structure from motion, i.e. to recover 3-D structure of objects from an image sequence.

In recent years, many techniques for the computation of optical flow have been proposed in literature. They can be classified into gradient-based, correlation-based, energy-based, and phase-based methods [2]. Among these methods, the gradient-based approach and the correlation-based approach are the two most popular ones.

The gradient-based approach is dependent on the image flow constraint equation, which is derived from the brightness constancy assumption as well as the first-order Taylor series approximation [5]. Using the image flow constraint equation alone is insufficient to compute the optical flow since each equation involves two different variables. Horn and Schunck [5] introduced a first order smoothness measure to constraint the flow field and solve for the flow. Since the smoothness constraint is invalid across the motion boundary, Nagel [9] proposed the "oriented smoothness" measure to suppress the smoothness constraint in the direction orthogonal to the boundaries.

Horn and Schunck's variational formulation of the optical flow problem [5] involves minimizing a combination of the optical flow constraint and a smoothness term. A discrete version of the energy to be minimized can be written as

$$\sum_i (E_{x,i}u_i + E_{y,i}v_i + E_{t,i})^2 + \frac{\lambda}{2}(u_{x,i}^2 + u_{y,i}^2 + v_{x,i}^2 + v_{y,i}^2) \quad (1)$$

Where, u_i and v_i form the discretized flow vector at the i-th pixel, $u_{x,i}, u_{y,i}, v_{x,i}$ and $v_{y,i}$ represent the discretized partials of the velocity field, $E_{x,i}$, $E_{y,i}$ and $E_{t,i}$ correspond to the discretized partials of the intensity function E at the i-th location in the x, y and t directions, respectively. The minimization of this discretized energy leads to solving a linear system $\mathbf{Ku} = \mathbf{b}$. The stiffness matrix $\mathbf{K} \in \Re^{2n^2 \times 2n^2}$ is symmetric positive-definite and has a sparsity structure.

Recently, Lai and Vemuri [7] proposed a modified gradient-based method for computing optical flow. The image flow constraint and a contour-based flow constraint are combined in a regularization framework to achieve accurate optical flow estimation. In addition, an incomplete Cholesky preconditioned conjugate gradient algorithm was proposed in [7] to minimize the energy function of the optical flow problem very efficiently. The incomplete Cholesky preconditioner is obtained by approximating the stiffness matrix $\mathbf{K}$ via an incomplete Cholesky factorization, preserves the sparsity of the matrix and leads to an efficient preconditioning technique.

The variation of an intensity function with time may be caused by geometric or photometric changes. The brightness constancy assumption, which is the basis for the derivation of the image flow constraint in the gradient-based approach, does not account for intensity variation due to photometric changes. A generalized brightness change model [10] has been proposed to generalize the gradient-based approach for the gradual time-varying illumination case. More recently, Zhang et al. [13] presented two methods for computing the optical flow under spatio-temporal non-uniform illumination. One is a spatio-temporal local optimization method and the other is a pixel-based temporal filtering method. Moreover, Nomura [11] proposed two generalized gradient-based methods for determining motion fields under non-stationary illumination. A non-stationary parameter was introduced in the generalized optical flow constraint to account for the illumination variation.

The correlation-based approach locally finds the displacement vector (u, v) between two images I_0 and I_1 at the location (x, y) by minimizing a sum of squared differences (SSD) function In this SSD function, the summation is performed in a window of size $(2k+1) \times (2k+1)$ centered at (x, y). Most correlation-based methods perform an extensive search for the displacement vector (u, v) in a finite integer-pair set and find the pair with the smallest SSD value as the solution displacement. Since the search region of the displacement vector is discretized for this extensive search, the accuracy of the computed optical flow is limited by this discretization. To obtain more reliable flow estimates over the entire image domain, Anandan [1] treated the estimates provided by the matching process as the data constraints for optical flow with appropriate confidence measure, and incorporated a smoothness constraint on the optical flow. Instead of applying smoothness constraints on the optical flow, Szeliski and Coughlan [12] used a two-dimensional spline model to represent the flow field and minimized the following SSD function

$$E(\mathbf{u}) = \sum_{j=1}^{n} \sum_{i=1}^{n} [I_1(i + u_{ij}, j + v_{ij}) - I_0(i, j)]^2 \quad (2)$$

where the vector $\mathbf{u}$ is the concatenation of the flow components u_{ij} and v_{ij}. A modified Levenberg-Marquardt algorithm was then employed to solve this non-convex optimization problem. They reported very accurate results using this method. The 2-D spline models for optical flow field assume the flow field to be well-approximated by the 2-D spline basis functions in the patches of a preset size.

In this paper, we use the standard finite difference discretization on the flow field and take a modified flow constraint as the data constraint energy in an adaptive regularization framework. We employ an incomplete Cholesky preconditioned conjugate gradient algorithm in conjunction with a coarse-to-fine strategy to efficiently minimize the total energy function. Experimental results on the standard synthetic image sequence using our algorithm compare favorably to the best existing results reported in literature. The proposed algorithm computes dense optical flow estimates from an image sequence and allows for the motion discontinuities to be incorporated.

The remainder of this paper is organized as follows. In the next section, we present the modified regularization formulation for optical flow computation from an image sequence. A numerical solution to the associated optimization problem is proposed in section 3. Experimental results for real image sequences are presented in section 4. Finally, we conclude in section 5.

2 A Modified Regularization Formulation

In this section, we present a new regularization formulation that alleviates the errors in the image flow constraint due to spatially-varying illumination changes for accurate optical flow computation. In addition to the geometric transformation (optical flow field), we introduce two new photometric functions, namely, illumination multiplication and illumination bias functions. The following equation is a modification of the brightness constancy assumption used in the traditional SSD approach

$$\begin{aligned} & I(x_i + u_i, y_i + v_i, t + \delta t) \\ = \; & \alpha(x_i, y_i, t) I(x_i, y_i, t) + \beta(x_i, y_i, t) \end{aligned} \quad (3)$$

The illumination multiplication function $\alpha(x, y, t)$ and the illumination bias function $\beta(x, y, t)$ are assumed to be smooth functions of the spatial coordinates. By taking the Laplacian operator ∇^2 on both sides of the equation, we can ignore the terms associated with the Laplacian of $\alpha(x_i, y_i, t)$ and $\beta(x_i, y_i, t)$, thus leading to the following equation

$$\nabla^2 I(x_i + u_i, y_i + v_i, t + \Delta t) = \alpha(x_i, y_i, t) \nabla^2 I_0(x_i, y_i, t) \quad (4)$$

If we neglect the factor $\alpha(x, y, t)$ in the Taylor series expansion of the above equation, then we have the new optical flow constraint equation as follows

$$(\nabla^2 I)_x u + (\nabla^2 I)_y v + (\nabla^2 I)_t = 0 \qquad (5)$$

Note that the proposed new optical constraint given in equation 5 involves the numerical approximation of third-order partial derivatives of the image intensity function I. In fact, the numerical computation of higher-order differentiation is very sensitive to noise. To alleviate the noise effect in the numerical approximation, we propose to use a Gaussian convolution in conjunction with the Laplacian operator in the above constraint to achieve more robust performance. Thus, the Laplacian operator in the constraint is replaced by a Laplacian of Gaussian (LoG) operator. The new equation is given as follows

$$((\nabla^2 G)I)_x u + ((\nabla^2 G)I)_y v + ((\nabla^2 G)I)_t = 0 \qquad (6)$$

where G is a Gaussian smoothing operator and $\nabla^2 G$ is a Laplacian of Gaussian operator. This data constraint can be further modified by using the normalized difference instead of the absolute difference by using a weighting function w_i for the new constraint at the location (x_i, y_i). This weighting function is given by

$$w_i = \frac{1}{\sqrt{((\nabla^2 G)I)_{x,i}^2 + ((\nabla^2 G)I)_{y,i}^2 + c}} \qquad (7)$$

where c is a constant used to avoid the error amplification at the locations with very small gradients, $((\nabla^2 G)I)_{x,i}$=$((\nabla^2 G)I)_x(x_i, y_i)$ and $((\nabla^2 G)I)_{y,i}$=$((\nabla^2 G)I)_y(x_i, y_i)$. The above normalization is used to approximate the minimum distance between the point (u_i, v_i) and the constraint plane $((\nabla^2 G)I)_{x,i}u_i + ((\nabla^2 G)I)_{y,i}v_i + ((\nabla^2 G)I)_{t,i} = 0$ by the normalized distance. This leads to a weighted optical flow constraint with the weight for each data constraint determined by the above normalization factor.

Incorporating the above new optical flow constraint into the regularization formulation, we obtain the total energy function

$$f(\mathbf{u}) = \sum_{i \in D} w_i \times \{((\nabla^2 G)I)_{x,i}u_i + ((\nabla^2 G)I)_{y,i}v_i + ((\nabla^2 G)I)_{t,i}\}^2 + \lambda(u_{x,i}^2 + u_{y,i}^2 + v_{x,i}^2 + v_{y,i}^2) \qquad (8)$$

where D is the set of all points in the image domain. Note the energy function to be minimized is quadratic and convex. This energy minimization can be accomplished by solving a symmetric positive definite (SPD) linear system. We use a preconditioned conjugate gradient method [4] with the incomplete Cholesky preconditioning to efficiently minimize this energy function in equation 8. In addition, a coarse-to-fine strategy can be employed to account for large-displacement problems and to accelerate the convergence rate of the preconditioned CG algorithm.

3 Preconditioned Conjugate Gradient Algorithm

The minimization of the above energy leads to solving a linear system of equations $\mathbf{Ku} = \mathbf{b}$ where the stiffness matrix $\mathbf{K} \in \Re^{2n^2 \times 2n^2}$ is symmetric positive-definite and it has the following 2×2 block structure.

$$\mathbf{K} = \begin{bmatrix} \lambda \mathbf{K}_s + \overline{\mathbf{E}}_{xx} & \overline{\mathbf{E}}_{xy} \\ \overline{\mathbf{E}}_{xy} & \lambda \mathbf{K}_s + \overline{\mathbf{E}}_{yy} \end{bmatrix}, \qquad (9)$$

where $\mathbf{K}_s \in \Re^{n^2 \times n^2}$ is the discrete 2-D Laplacian matrix from the membrane smoothness constraint, $\overline{\mathbf{E}}_{xx}$, $\overline{\mathbf{E}}_{xy}$, and $\overline{\mathbf{E}}_{yy}$ are all $n^2 \times n^2$ diagonal matrices with entries $\overline{I}_{x,i}^2 + \overline{S}_{x,i}^2$, $\overline{I}_{x,i}\overline{I}_{y,i} + \overline{S}_{x,i}\overline{S}_{y,i}$ and $\overline{I}_{y,i}^2 + \overline{S}_{y,i}^2$, respectively. Note that the values of $\overline{I}_{x,i}$ and $\overline{I}_{y,i}$ are set to zeros when the image flow constraint is disabled at the i-th location due to reliability measure test. Similarly, the values of $\overline{S}_{x,i}$ and $\overline{S}_{y,i}$ are set to zeros when the contour flow constraint is not used at the i-th location.

To solve this linear system for optical flow estimation, we use the preconditioned conjugate gradient algorithm [4] with an incomplete Cholesky preconditioner $\mathbf{P}$ [8, 3], given in the following.

1. Initialize $\mathbf{u}_0$; compute $\mathbf{r}_0 = \mathbf{b} - \mathbf{K}\mathbf{u}_0$; $k = 0$.
2. Solve $\mathbf{P}\mathbf{z}_k = \mathbf{r}_k$; $k = k + 1$.
3. If $k = 1$, $\mathbf{p}_1 = \mathbf{z}_0$; else compute $\beta_k^D = \mathbf{r}_{k-2}^T \mathbf{z}_{k-2}$, $\beta_k = \frac{\alpha_{k-1}^N}{\beta_k^D}$, and update $\mathbf{p}_k = \mathbf{z}_{k-1} + \beta_k \mathbf{p}_{k-1}$.
4. Compute $\alpha_k^N = \mathbf{r}_{k-1}^T \mathbf{z}_{k-1}$, $\alpha_k^D = \mathbf{p}_k^T \mathbf{K} \mathbf{p}_k$, and $\alpha_k = \alpha_k^N / \alpha_k^D$;
5. Update $\mathbf{r}_k = \mathbf{r}_{k-1} - \alpha_k \mathbf{K} \mathbf{p}_k$, $\mathbf{u}_k = \mathbf{u}_{k-1} + \alpha_k \mathbf{p}_k$.
6. If $\mathbf{r}_k \simeq \mathbf{0}$, stop; else go to step 2.

The incomplete Cholesky preconditioning has been successfully applied in the gradient-based approach for computing optical flow to efficiently solve the large and sparse linear system with the specially structured stiffness matrix [7, 6]. This preconditioner is very efficient since the incomplete Cholesky decomposition was performed to approximate the large and sparse stiffness matrix by exploiting its special structure. This preconditioning technique is used in conjunction with the conjugate gradient algorithm to minimize the energy function given in equation 8. With this preconditioning, the convergence of the conjugate gradient algorithm can be speeded up dramatically.

The preconditioner $\mathbf{P}$ is chosen as the incomplete Cholesky factorization of the matrix $\mathbf{K}$. A good preconditioner can drastically accelerate the convergence rate of the conjugate gradient algorithm. There are two criteria for designing a good preconditioner $\mathbf{P}$ for the matrix $\mathbf{K}$. First, the preconditioner $\mathbf{P}$ has to be a good approximation to $\mathbf{K}$ so that the condition number of the preconditioned linear system is dramatically reduced. Secondly, there must exist a very fast numerical method to solve the auxiliary linear system $\mathbf{Pz} = \mathbf{r}$ required in the preconditioned CG algorithm. Taking these two criteria into consideration, a good preconditioner for the above stiffness matrix $\mathbf{K}$ of the optical flow problem can be obtained via the incomplete Cholesky factorization of $\mathbf{K}$.

The standard Cholesky factorization of the sparse matrix $\mathbf{K}$ "fills in" entries in the band between nonzero off-diagonals, which means the sparsity structure will be destroyed after the factorization. The idea of incomplete Cholesky factorization is to find an approximate Cholesky factorization of the matrix $\mathbf{K}$, i.e. $\mathbf{K} \approx \mathbf{L}\mathbf{L}^T$, such that the lower triangular matrix $\mathbf{L}$ has the similar sparsity structure. In addition, the product $\mathbf{L}\mathbf{L}^T$ at the locations with nonzero entries in $\mathbf{L}$ or $\mathbf{L}^T$ still has the same values as those in $\mathbf{K}$. Therefore, the preconditioner $\mathbf{P} = \mathbf{L}\mathbf{L}^T$ is a good approximation to $\mathbf{K}$. Since the matrix $\mathbf{K}$ is sparse and well-structured, the matrix $\mathbf{L}$ is also sparse and well-structured. Thus, the solution to the auxiliary linear system $\mathbf{Pz} = \mathbf{r}$ in the preconditioning step of the preconditioned conjugate gradient algorithm can be obtained via forward and backward substitutions very efficiently. Furthermore, we use the block version [4] of the incomplete Cholesky factorization to take advantage of the 2×2 block structure of the matrix $\mathbf{K}$.

The matrix $\mathbf{K}$ in equation 9 has diagonal blocks $\lambda \mathbf{K}_s + \overline{\mathbf{E}}_{xx}$ and $\lambda \mathbf{K}_s + \overline{\mathbf{E}}_{yy}$, each of which is block tridiagonal. The off-diagonal elements of $\mathbf{K}$ are diagonal blocks, each of which is a diagonal matrix. In addition, the off-diagonal elements of the block tridiagonal matrices $\lambda \mathbf{K}_s + \overline{\mathbf{E}}_{xx}$ and $\lambda \mathbf{K}_s + \overline{\mathbf{E}}_{yy}$ are diagonal. The factoring matrix in the incomplete Cholesky factorization has the similar sparse structure as that of $\mathbf{K}$ and takes the following form.

$$\mathbf{L} = \begin{bmatrix} \mathbf{L}_{11} & \mathbf{0} \\ \mathbf{L}_{21} & \mathbf{L}_{22}, \end{bmatrix} \qquad (10)$$

where the sub-matrices $\mathbf{L}_{11}$, $\mathbf{L}_{21}$ and $\mathbf{L}_{22}$ are of size $n^2 \times n^2$. Our incomplete Cholesky factorization is based on the construction of an incomplete block preconditioner in [4]. The sub-matrices $\mathbf{L}_{11}$, $\mathbf{L}_{22}$ and $\mathbf{L}_{21}^T$ are chosen to be block lower bidiagonal matrices with the diagonal blocks being lower bidiagonal and the lower diagonal blocks being upper bidiagonal, i.e., the matrices $\mathbf{L}_{11}$, $\mathbf{L}_{22}$ and $\mathbf{L}_{21}$ have the following structures,

$$\mathbf{L}_{ij} = \begin{bmatrix} \mathbf{G}_{ij}^{(1)} & & & \\ \mathbf{H}_{ij}^{(1)} & \mathbf{G}_{ij}^{(2)} & & \\ & \ddots & \ddots & \\ & & \mathbf{H}_{ij}^{(n-1)} & \mathbf{G}_{ij}^{(n)} \end{bmatrix}, \qquad (11)$$

for $(i,j) \in \{(1,1),(2,2)\}$, and

$$\mathbf{L}_{21} = \begin{bmatrix} \mathbf{G}_{21}^{(1)^T} & \mathbf{H}_{21}^{(1)^T} & & \\ & \mathbf{G}_{21}^{(2)^T} & \ddots & \\ & & \ddots & \mathbf{H}_{21}^{(n-1)^T} \\ & & & \mathbf{G}_{21}^{(n)^T} \end{bmatrix}, \qquad (12)$$

where

$$\mathbf{G}_{ij}^{(k)} = \begin{bmatrix} \alpha_{ij,1}^{(k)} & & & \\ \beta_{ij,1}^{(k)} & \alpha_{ij,2}^{(k)} & & \\ & \ddots & \ddots & \\ & & \beta_{ij,n-1}^{(k)} & \alpha_{ij,n}^{(k)} \end{bmatrix} \in \Re^{n \times n},$$

$$\mathbf{H}_{ij}^{(k)} = \begin{bmatrix} \gamma_{ij,1}^{(k)} & \delta_{ij,1}^{(k)} & & \\ & \gamma_{ij,2}^{(k)} & \ddots & \\ & & \ddots & \delta_{ij,n-1}^{(k)} \\ & & & \gamma_{ij,n}^{(k)} \end{bmatrix} \in \Re^{n \times n},$$

for $k = 1, \ldots, n$. The nonzero entries in the sparse matrix $\mathbf{L}$ are computed by equating the entries of the product $\mathbf{L}\mathbf{L}^T$ to those in the matrix $\mathbf{K}$ at the locations with nonzero entries in $\mathbf{L}$. Thus, the nonzero entries in $\mathbf{L}_{11}$, $\mathbf{L}_{21}$ and $\mathbf{L}_{22}$ are given in [7, 6].

The incomplete Cholesky factorization of the matrix $\mathbf{K}$ given above can be computed in $O(N)$ operations, where $N (= n^2)$ is the number of discretization points. After the factorization, the preconditioner $\mathbf{P}$ is chosen as $\mathbf{L}\mathbf{L}^T$, which is close to $\mathbf{K}$ and has a nice structure. Thus, the preconditioned conjugate gradient algorithm requires $O(N)$ operations in each iteration.

The incomplete Cholesky preconditioning has been used to greatly improve the convergence speed of the conjugate gradient algorithm for the optical flow computation problem [7]. In addition, it is very efficient since it only requires $O(N)$ operations in each iteration.

4 Experimental Results

In this section, we present results of testing the proposed modified regularization algorithm on a variety image sequences. Unlike some other methods which only produce sparse optical flow, the proposed algorithm give dense optical flow estimates with 100% density. The experimental results of using the proposed regularization method on two synthetic and two real image sequences are presented here. The two synthetic image sequences are the *Translating Tree* and the *Yosemite* image sequences. Our results on these two examples are compared to the best optical flow estimates reported in literature.

(a)

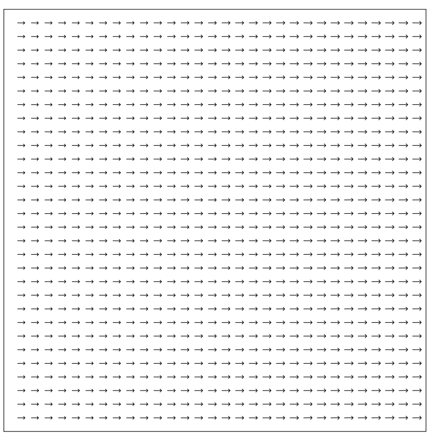

(b)

Figure 1: (a) One frame from the *Translating Tree* sequence and (b) the computed optical flow using the proposed algorithm.

In our implementation, a coarse-to-fine strategy is combined with the preconditioned conjugate gradient algorithm to find the minimum energy solution. Three resolutions are used in the coarse-to-fine strategy and 20 iterations of the preconditioned conjugate gradient algorithm are computed for each resolution. By using the coarse-to-fine strategy, we can deal with large displacement problems with better convergence property during the solution search. The regularization parameter λ is empirically chosen to be 0.5 for the implementation of the proposed regularization method. The results are quite stable for the regularization parameter in the range between 0.1 and 1. The constant c in the normalization factor was set to 0.01 for all the experiments presented in this paper.

For the translating tree example, each frame contains more complicated highly textured regions, which result in multiple local minima in the associated energy function to be minimized. One frame of the image sequence is shown in Fig. 1(a). The computed optical flow is shown in Fig. 1(b). Our proposed regularization method compares favorably to the best existing methods in this example.

Technique	Avg. Error	Std.	Density
Horn & Schunck (modified)	$2.02°$	$2.27°$	100%
Uras et al.	$0.62°$	$0.52°$	100%
Szeliski & Coughlan	$0.35°$	$0.34°$	100%
Lucas & Kanade ($\lambda_2 \geq 5.0$)	$0.56°$	$0.58°$	13.1%
Weber & Malik	$0.49°$	$0.35°$	96.8%
Fleet & Jepson	$0.23°$	$0.19°$	49.7%
Lai	$0.35°$	$0.30°$	100%

Table 1: Summary of *Translating Tree* results

We also tested our algorithm on the *Yosemite* sequence. We compared our modified regularization method with the other methods for the *Yosemite* sequence. Three frames of the sequence and the correct flow field are shown in Figure 2. From the images, we can observe the image intensity variations in sky region of the sequence involve non-uniform illumination changes, i.e. the brightness constancy assumption is not valid in this case. Several previous methods have reported results on this sequence ignoring the sky region. A summary of the reported results including the result using the proposed algorithm is given in Table 2 for comparison. The sign "*" followed by a method indicates that the error was computed without the sky region. It is obvious that our modified regularization method compare favorably to the best existing methods in this example.

In addition to the above accuracy comparison, we depict the computed optical flow fields using the proposed algo-

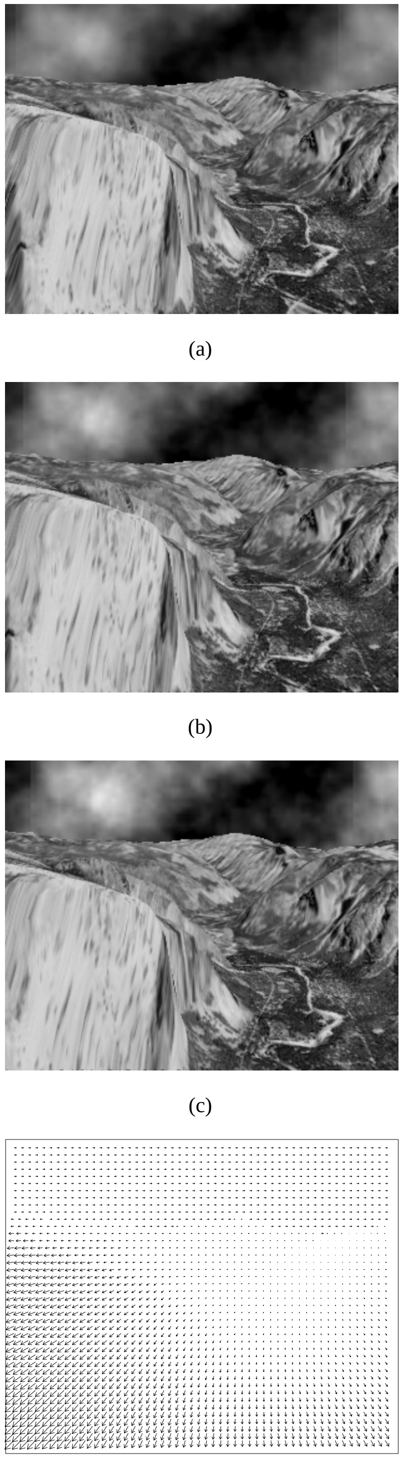

(a)

(b)

(c)

(d)

Figure 2: The (a) 6-th, (b) 9-th and (c) 12-th frames from the *Yosemite* image sequence and (b) the true optical flow field.

Technique	Avg. Error	Std.	Density
Horn & Schunck (modified)	9.78°	16.19°	100%
Uras et al.	8.94°	15.61°	100%
Black & Anandan*	4.46°	4.21°	100%
Szeliski & Coughlan*	2.45°	3.05°	100%
Black & Jepson*	2.29°	2.25°	100%
Ju et al.*	2.16°	2.0°	100%
Lai & Vemuri *	1.99°	1.41°	100%
Lai & Vemuri	7.81°	14.57°	100%
Zhang et al.	5.59°	11.24°	100%
Lai*	2.05°	1.61°	100%
Lai	5.19°	9.27°	100%

Table 2: Summary of *Yosemite* results

rithm and a previous improved gradient-based algorithm [7] in Figure 3 to demonstrate the performance of the proposed algorithm under non-uniform illumination variations. From the figure, we can see the previous gradient-based method suffers from the non-uniform illumination variations in the sky region, while the proposed algorithm based on the conservation of the LoG filter intensity produced accurate estimation all over the image domain.

Finally, the proposed regularization method was applied to a real image sequences namely the *Hamburg Taxi* sequence. Figure 4 depicts the experimental result on the *Hamburg Taxi* sequence.

5 Conclusion

In this paper, we presented a new modified regularization method for computing optical flow from an image sequence. We derived a new flow constraint based on a generalized brightness assumption and by taking a Laplacian of Gaussian operation on the image. Then the new flow constraint is appropriately normalized and combined with the membrane smoothness in a regularization framework. The resulting energy function is quadratic and convex. The incomplete Cholesky preconditioned conjugate gradient algorithm was employed to minimize this energy function. We have obtained very accurate results by applying this algorithm to compute optical flow for several image sequences. Also, we have experimentally demonstrated that our algorithms for optical flow computation compare favorably to all the best existing methods reported to date in literature. The future work will focus on extending the regularization framework presented here to allow for motion discontinuity by modifying the smoothness assumption to adaptive smoothing.

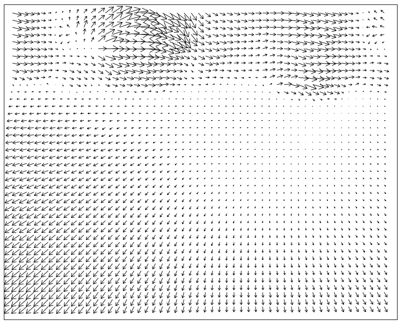

(a)

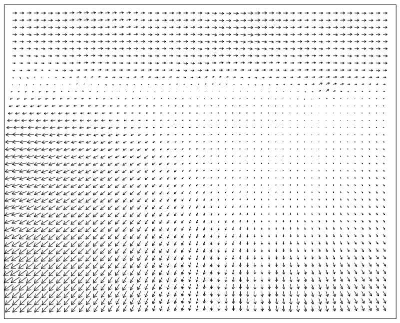

(b)

(c)

(d)

Figure 3: The computed optical flow fields using (a) the modified Horn and Schunck's method and (b) the proposed regularization method for the *Yosemite* image sequence. The optical flows overlaid on the image are shown in (c) and (d), respectively.

(a)

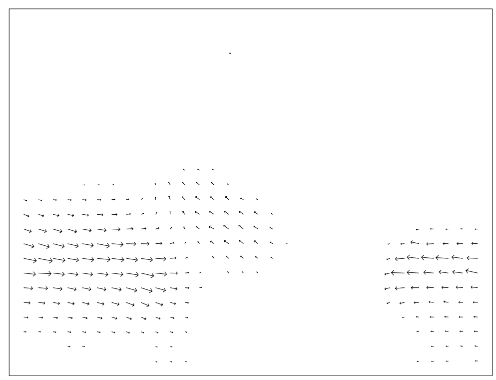

(b)

Figure 4: (a) One frame from the *Hamburg Taxi* sequence. (b) Computed optical flow using the proposed modified regularization method after 50 iterations of the preconditioned conjugate gradient algorithms.

Acknowledgments

The author would like to thank National Science Council, Taiwan, R.O.C., for supporting this research under the grant NSC 89-2213-E-007-097.

References

[1] P. Anandan. A computational framework and an algorithm for the measurement of visual motion. *International Journal of Computer Vision*, 2:283–310, 1989.

[2] J. L. Barron, D. J. Fleet, and S. S. Beauchemin. Performance of optical flow techniques. *International Journal of Computer Vision*, 12(1):43–77, 1994.

[3] H. C. Elman. A stability analysis of incomplete LU factorizations. *Mathematics of Computation*, 47(175):191–217, 1986.

[4] G. H. Golub and C. F. Van Loan. *Matrix Computations*. The Johns Hopkins University Press, 2nd edition, 1989.

[5] B. K. P. Horn and B. G. Schunck. Determining optical flow. *Artificial Intelligence*, 17:185–203, 1981.

[6] S.-H. Lai. Incomplete Cholesky preconditioning for early vision. In *Proc. the Fourth Asian Conference on Computer Vision*, pages 318–323, Taipei, Taiwan, 2000.

[7] S.-H. Lai and B. C. Vemuri. Reliable and efficient computation of optical flow. *International Journal of Computer Vision*, 29:87–105, 1998.

[8] J. A. Meijerink and H. A. van der Vorst. An iterative solution method for linear systems of which the coefficient matrix is a symmetric M-matrix. *Mathematics of Computation*, 31(137):148–162, 1977.

[9] H.H. Nagel and W. Enkelmann. An investigation of smoothness constraints for the estimation of displacement vector fields from image sequences. *IEEE Trans. Patt. Anal. Mach. Intell.*, PAMI-8(5):565–593, Sept. 1986.

[10] S. Negahdaripour and C. Yu. A generalized brightness change model for computing optical flow. In *Proc. International Conference on Computer Vision*, pages 2–11, Berlin, Germany, 1993.

[11] A. Nomura. Spatio-temporal optimization method for determining motion vector fields under non-stationary illumination. *Image and Vision Computing*, 18:939–950, 2000.

[12] R. Szeliski and J. Coughlan. Hierarchical spline-based image registration. In *Proc. IEEE Conference on Computer Vision Pattern Recognition*, pages 194–201, Seattle, Washington, 1994.

[13] L. Zhang, T. Sakurai, and H. Miike. Detection of motion field under spatio-temporal non-uniform illumination. *Image and Vision Computing*, 17:309–320, 1999.